Understanding the Semi-switchable Thermochromic Behavior of Mixed Halide Hybrid Perovskite Nanorods

Anurag Roy,* Habib Ullah, Aritra Ghosh, Hasan Baig, Senthilarasu Sundaram, Asif Ali Tahir, Tapas K. Mallick*

Environment and Sustainability Institute, University of Exeter, Penryn Campus, Cornwall TR10 9FE, U.K.

ABSTRACT

Intelligent regulation of solar irradiation and modulation of a window's thermo-optical properties can be achieved using thermochromic (TC) coating implementation. In this work, the semi-switchable TC property of a mixed halide hybrid perovskite, $CH_3NH_3PbI_{3-x}Br_x$, has been thoroughly investigated from the bromine addition as x = 0, 1, 2, 3, perspective. The composition of $CH_3NH_3PbIBr_2$ (when x = 2) nanorods exhibits excellent TC behavior, and further explores TC coating material for smart window application. An attempt has been forged to establish a structure-property-performance relationship for a TC perovskite window, engaging various physicochemical characterizations. The TC perovskite nanorods exhibit a significantly low-temperature transition thermochromism in the visible and ultraviolet region. TC properties further escalate in the visible light transmittance (T_{vis}) and solar modulation (T_{sol}). The first-principles calculations involving density of states, crystal structure, band alignment, and thermochromic behaviour interpretation of $CH_3NH_3PbIBr_2$ further confirms effectively separating the crystal structure alignments once in contact with water driving their TC characteristics. Intriguing the perovskite smart window can anticipate reducing the indoor air temperature by about 50°C when the outside temperature reaches 80ºC. This work's combined experimental and theoretical approach expressly offers a preliminary attempt to develop and design strategies that seek to balance thermal and luminous spaces served by glazing integrated nanostructured perovskite material systems.

1. INTRODUCTION

Recently, organic-inorganic hybrid halide perovskite of an ABX_3 structure [$A = CH_3NH_3^+$ (MA), $HC(NH_2)_2^+$ (FA), Cs^+; $B = Pb^{2+}$, Sn^{2+}; $X = I^-$, Br^-, Cl^-] appeared as a potential absorber and fashionable for perovskite solar cells (PSCs) and manifested their outstanding contribution among the photovoltaic (PV) technologies.[1,2] The most efficient PSCs are fabricated using $CH_3NH_3PbI_3$ ($MAPbI_3$) or analogous mixed cation lead-based hybrid halide perovskites. Researchers are interested in analyzing $MAPbI_3$ for energy-saving building and glazing to become an intriguing optical, thermal, and electrical property. This functionality prescribes chromogenic materials whose characteristic feature is responding persistently and reversibly to external stimuli. For window application, semitransparency and thermo-chromaticity are preconditions, as natural daylight penetrating through this semitransparency and thermo-chromaticity creates a comfortable indoor environment. The thermochromic (TC) coating was employed in several studies to replace the traditional window at homes or buildings. Bastiani et al. (2017) reported the excellence of MAPbBrI, a mixed halide hybrid perovskite's TC behavior for the window.[3] A completely reversible chromatic variation ranging from yellow to black as the temperature increases from 25 to 120 °C was achieved. Another hybrid material, $FA_{n+1}Pb_nX_{3n+1}$ (FA = formamidinium, X = I, Br; n = number of layers = 1, 2, 3 … ∞), reversibly switch between their tunable colours.[4] Recently, Zhang et al. (2019) performed a variation of PbI_2 and I mixing ratio and analyze their respective TC behaviour.[5] Their results varied between 34.3% and 59.6% for luminous transmittance in the hot state and between 12.7% and 25.5% for solar modulation ability during the variation of PbI_2 and MA to form $MAPbI_3$. The photothermal heating switching behavior of $MAPbI_3$ perovskite was also observed by Wheeler et al. (2017).[6] On the other hand, the TC properties are strongly correlated to structure and morphology.[7] For a mixed halide perovskite, halide segregation into

iodide-rich minority and bromide-enriched majority domains was influenced by a low energy photoluminescence feature, the optical properties of the perovskite.[8] Substituting iodide by bromide can tune the bandgaps of $MAPbI_3$ in the range between 1.5 to 2.2 eV by sequential bromine incorporation to get $MAPbBr_3$.[9]

Thin coating of one-dimensional (1D) morphologies, such as nanorod, nanowire hold great promise because of their high diffuse reflectance, optical transmittance and anisotropic thermal behavior, simultaneously provide good optimization of a trade-off between transparency and structural continuity.[10,11] Study on window material's morphology depended TC behavior is limited. Therefore, we find that the impact of 1D perovskite TC on glazing performance is still lacking and requires analyzing their thermal performance and energy efficiency when subjected to varying climate conditions. In TC coating for window, vanadium dioxide (VO_2) becomes the leading candidate due to its first-order phase transition from a monoclinic semiconducting state to a tetragonal metallic at a transition temperature (T_t) 68^{o}C.[12,13] Besides, VO_2 can intelligently adjust the near-infrared (NIR) radiation according to the environmental temperature.[14-18] Besides, as an organic hydrogel, crosslinked poly(N-isopropyl acrylamide) or PNIPAm, a typical temperature-responsive hydrogel combined with graphene oxide was employed for a switchable glazing and adaptive solar control.[4] However, despite the growing interest and potential advantages, state-of-the-art TCs suffer from limiting their comprehensive utilization, such as narrow chromatic variation, high operating temperature, and UV-light instability. This work further indicates an apparent effort towards perovskite integration in window applications besides their emerging PV application. This study tried to establish the optical and thermal behavior of semi-switchable thermochromic mixed halide perovskite's, consisting of a low T_t. This behavior is very promising for the occupants' visual comfort and energy-efficient windows in buildings. The primarily used

hybrid perovskite $MAPbI_3$ is very unstable in the open environment as it degrades rapidly in a humid climate supported by ultraviolet light. To counter this problem, researchers are incorporating other halides (bromine, chlorine) in $MAPbI_3$. The incorporation of bromine enhances the stability of the material, but it also increases the bandgap. Bromine addition reduces the charge recombination resulted in improving the optical property.[19,20]

Switchable material for window application is of utmost importance because the building sector consumes 40% of global fossil fuel-generated energy. While there is an extensive no switchable material for building window application under investigation, very few achieved the desired outcome. Switchable material will thermal actuation has a notable positive impact as there is no external power supply requirement. Hence, our effort significantly influences TC perovskite material integration followed by a sequential relationship establishment of structure-property-performance relationship to utilize it for building window purposes. In this present study, an effort has been executed to understand the TC behaviour of a hybrid mixed halide perovskite, $MAPbI_{3-x}Br_x$, to interpose the current window materials. A one-pot synthesis technique has been adopted to produce $MAPbIBr_2$ nanorods, which excels impressively semi-switchable or irreversible TC behaviour from yellow (22^{o}C) to maroon (60^{o}C), consisting comparability lower T_t (40^{o}C), and offering enhanced stability and reproducibility.

Furthermore, the TC coating purveys a maximum temperature difference of 50^{o}C when the outside temperature reaches 80^{o}C. However, state-of-the-art TCs suffer from limiting their comprehensive utilization, such as narrow chromatic variation, high operating temperature, and UV-light instability despite the growing interest and potential advantages. Our findings promise morphology oriented semi-switchable thermochromic property evaluation for a mixed halide perovskite's, consisting of a low transition temperature and efficient candidate for window high-temperature

thermal comfort. Apart from that, this work further indicates an apparent effort towards perovskite integration in window applications along with their potential PV application.

2. EXPERIMENTAL SECTION

2.1. Synthesis of $CH_3NH_3PbIBr_2$. The oleate-chelation method employed the $MAPbI_{3-x}Br_x$ perovskite nanorods to be synthesized through the colloidal synthesis approach (hot-injection method).[21,22] A typical colloidal synthesis scheme has been given in **Figure 1**. In this study, the $MAPbI_{3-x}Br_x$ was synthesized by varying the iodide-bromide ratio (x) from 0.0 to 3.0 with an increment of 1.0. Four (x = 0, 1, 2, 3) mixed halide hybrid perovskite ($MAPbI_{3-x}Br_x$) samples with different x values have been prepared. In detail, to prepare $MAPbIBr_2$, 0.576 g of PbI_2 was mixed with 0.556 g of MAI in 2 mL oleic acid (OA) and 25 ml octadecene (ODE) in a 100 ml three-necked flask with magnetic stirring and then heated to 120℃ for half an hour under N_2 environment. Besides, 0.917 g of $PbBr_2$ was dissolved in 5 mL of anhydrous γ-Butyrolactone, and then quickly injected into the three-necked flask and then heated to 135℃ to keep half an hour until the solution turned into bright yellow. Finally, the $MAPbI_{3-x}Br_x$ nanorods were obtained. The nanorods were purified using 2 mL of dimethylformamide (DMF) to resolve the unreacted OA and ODE. Pure nanorods were obtained after several purifications. Further, the synthesized nanorods were dispersed in DMF for their coating development. A layer of as-prepared perovskite solution was employed to develop the coating on a 5 cm x 5 cm low-iron glass by spin-coating (SPIN-1200D, Midas System) at 1500 rpm for 30 sec (**Figure 1**).

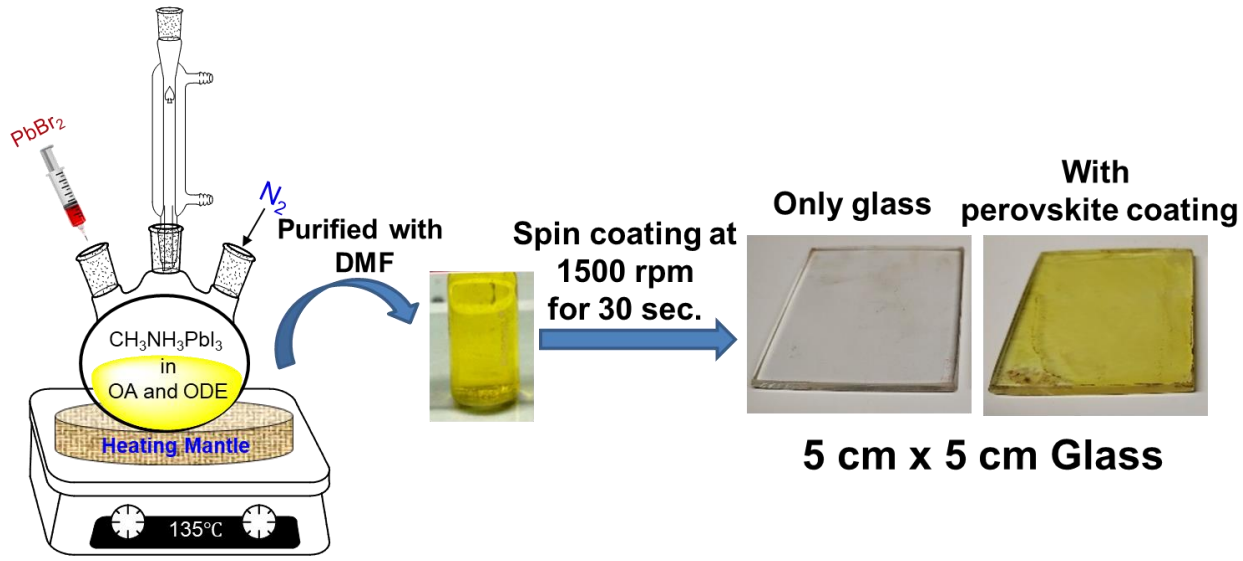

Figure 1. Synthesis of $MAPbI_{3-x}Br_x$ perovskite solution by the hot-injection method and photographs corresponding film fabricated by the spin-coating method.

2.2. Glazing Characterization. The fabricated perovskite coatings were thermally treated across a temperature window, starting from room temperature (22^{o}C), and increased with an interval of 5^{o}C up to 60 ^{o}C. The temperature was not further raised >60^{o}C, as no significant optical or structural change was observed unless PbI_2 production. Similarly, we were unable to lower the temperature < 22^{o}C, as at lower temperature, the perovskite absorbs inflated moisture resulting in degradation and thus becomes opaque. Therefore, in this study, we observed the perovskite coating's thermal characteristics at a higher temperature. The thermal treatment of transmittance measurement, thermochromic kinetics, and cycle testing was carried out using a hot plate. In contrast, the temperature profile experiment was executed under the 1 SUN 1.5 AM.

A similar experimental set-up was adopted from our previous publications to understand the glazing temperature profile under 1 SUN 1.5 AM of the fabricated perovskite coating.[23, 24] In short, a small-scale test cell dimension of 5 cm x 5 cm x 5 cm definitive three-dimensional (3D) printed prototype chamber was fabricated using 10 mm thick polystyrene to perform indoor

characterization. The ratio of test cell and window was 1:1. Outdoor characterization using a test cell simultaneously offers several constraints and internal and external variables.

The value of luminous transmission (T_{Vis}) can be acquired from equations (i) and (ii)[24]

Luminous transmission or reflection $T_{Vis} = \frac{\sum_{\lambda=380\ nm}^{780\ nm} y(\lambda)T(\lambda)\Delta\lambda}{\sum_{\lambda=380\ nm}^{780\ nm} y(\lambda)\Delta\lambda}$ (i)

Solar transmission $T_{sol} = \frac{\sum_{\lambda=200nm}^{2000nm} A,M1.5(\lambda)T(\lambda,\alpha)\Delta\lambda}{\sum_{\lambda=200nm}^{2000nm} A.M1.5(\lambda)\Delta\lambda}$ (ii)

Where T (λ) is the transmittance of the TC perovskite coating windows at wavelength λ, the CIE (International Commission on Illumination) standards for photopic luminous efficiency of the human eye (y(λ)) and the solar irradiance spectrum for an air mass of 1.5 (AM1.5 (λ)) were used as weighting functions for the wavelength-dependent transmittance. T_{Vis} is 380 nm≤ λ≤ 780 nm corresponding to human vision limits. The standard test conditions (STC) correspond to an irradiance of 1000W/m^2, an AM (air mass) 1.5 spectrum and a device temperature of 22°C.[25]

2.3. Material Characterization. The transmittance, absorbance spectra of the perovskite coating samples were measured using the LAMBDA 1050 UV/Vis/NIR spectrophotometer, Perkin Elmer, from 200-2000nm. X-ray diffraction (XRD) analysis was characterized by BRUKER D8 Advance X-ray diffractometer (Cu Kα irradiation, 40 kV/40 mA, 0.02° 2θ step size and a scan time of 3 s per step) in the range of 5-60°. The scanning electron microscopy (SEM) images and Energy Dispersive X-Ray Analysis (EDX) of the perovskite coating samples was analyzed on a TESCAN VEGA3 SEM. The prototype chamber's temperature profile was measured under 1000 W.m^{-2} (1 SUN 1.5 AM) of light from a WACOM AAA+ continuous solar simulator (model WXS-210S-20)56. Temperature recording was performed using the TC-08 thermocouple data logger (Pico Technology).[26]

3. THEORY AND COMPUTATIONAL DETAILS

Density functional theory (DFT) simulations were performed on Quantum-ATK[1]. The results were visualized on VNL Version 2019.12.[27] In order to validate our experimental data; we modelled the tetragonal unit cell of $MAPbI_3$ with a space group of 14/mcm, lattice parameters a = b =8.4822 Å, c = 11.9944 Å, followed by its 2 x 2 x 2 supercell. We used three types of models in this work, i.e., pure $MAPbI_3$, 2%-Br-doped $MAPbI_3$ ($MAPbIBr_2$), and $MAPbBr_3$. The two-dimensional (2D) slabs of $MAPbI_3$, $MAPbIBr_2$) and $MAPbBr_3$ along [001] direction is constructed to predict the effect of water/moisture, where two molecules of water have interacted on their surfaces (*vide infra*). The interaction of the water molecule is calculated with the help of equation (iii).

$$\Delta E_{\text{ad}} = E_{\text{surface@}H_2\text{O}} - (E_{H_2\text{O}} + E_{\text{surface}}) \qquad \text{(iii)}$$

$E_{surface@H2O}$ is the total energy of water interacted species, E_{H2O} is the energy of water molecule, and E_{suface} is the total energy of bare $MAPbIBr_2$(001). The linear combination of atomic orbitals (LCAO) has been employed for the N, C, H, I, Br, O, and Pb atoms. Generalized gradient approximation (GGA) with the Perdew-Burke-Ernzerhof (PBE) exchange-correlation functional and double Zeta Polarized (DZP) basis set is used for the structural and energy optimization.[28] A 4x4x3 Monkhorst-Pack k-grid and energy cutoff of 1200 eV is used for the bulk of $MAPbI_3$ and its doped species. The band structure, electrostatic potential (ESP), electron difference density, the density of states (DOS), and partial DOS (PDOS) calculations were simulated at FHI functional with the DZP basis set.

4. RESULTS AND DISCUSSION

4.1. Optoelectronics and Thermochromic Property Evaluation of the Perovskite Film. As bromine addition directly affects the optical bandgap of the mixed halide perovskite, which was further evaluated in **Figure 2a**. Variation of bromine incorporating (x) resulted in a hypsochromic shift of the sharp absorption edge of the perovskite as shifted from x=0 to 3, and further extracted from diffused reflectance spectra using the Kubelka-Munk (K-M) equation, $\alpha/s = [1-R]^2/2R$, where α and S are the absorption and scattering coefficient, respectively, and R is the reflectance.[19] Further, the bandgap value as observed from the K-M plot was calculated to be 1.35, 1.64, 1.88, and 2.1 eV for x = 0.0, 1.0, 2.0, and 3.0, respectively. In **Figure 2b**, it is perceptible that the band gaps are gradually increasing with x, confirming good tunability. The bandgap varies in almost linear fashion composition. The small variation in the band gaps compared to the other report may arise from the difference in particle sizes or morphology of the reaction yields. The diverse TC colour image has been given in **Figure 2c**, which signifies good color tunability of the samples with the increment of bromide. The diverse colour image exhibits the importance of mixed halide integration for perovskite development in their distinct reversible colour variation and lower T_t. The composition $MAPbIBr_2$ shows distinct colour variation followed by reversible TC colour tunability among the composition of the other. A discreet color difference was observed on changing the temperature in the case of $MAPbI_2Br$ or $MAPbBr_3$; however, they did not show reversible TC behaviour. Thus, we were further interested in dealing only with the sample, $MAPbI_2Br$, as it shows switchable TC among the other composition.

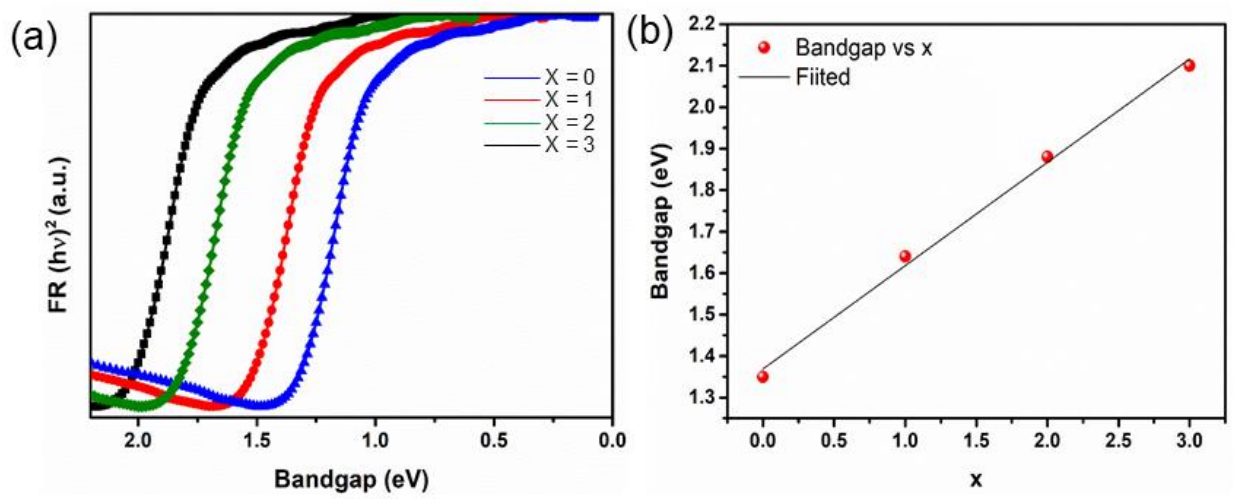

(c)

	22°C	30°C	45°C	55°C	TC Behaviour
VO_2					Non-reversible
$MAPbI_3$ X=0					Non-reversible
$MAPbI_2Br$ X=1					Non-reversible
$MAPbI_1Br_2$ x = 2					Semi-Reversible
$MAPbBr_3$ x = 3					Non-reversible

Figure 2. (a) Kubelka-Munk plot to calculate band gaps, (b) bandgap vs x., and (c) diverse thermochromic colour images of the samples.

The transmission spectra were recorded against various temperatures, as shown in **Figure 3a**. Variation of the perovskite coating's surface thermal treatment exhibits a gradual change in their respective optical transmittance. As demonstrated from **Figure 3a**, the perovskite coating exhibits high transparency of ~92% at 22°C. Once the temperature started to increase, a steady reduction in transparency is observed. After 40°C, the optical transparency of the coating drastically changed. At 60°C, the visible transparency (T_{vis}) dropped to 30%, followed by a spectra's bathochromic shifting. Besides, an unintentional shifting of the visible band transmittance of

spectra is observed, indicating perovskite degradation offered at higher temperature and moisture contact. During the coating surface temperature reduction to 22°C, there is an improvement of transparency spotted. The maximum transparency was found 48% at 800 nm once the temperature switched to 22°C. Also, during the coating's thermal treatment, it is observed that $T_{NIR} > T_{vis}$ at a higher temperature, even after switching temperature (**Figure 3b**). Besides the optical transmittance changing, there is a gradual colour change of the perovskite coating observed, as shown in the photographs of **Figure 3c**.

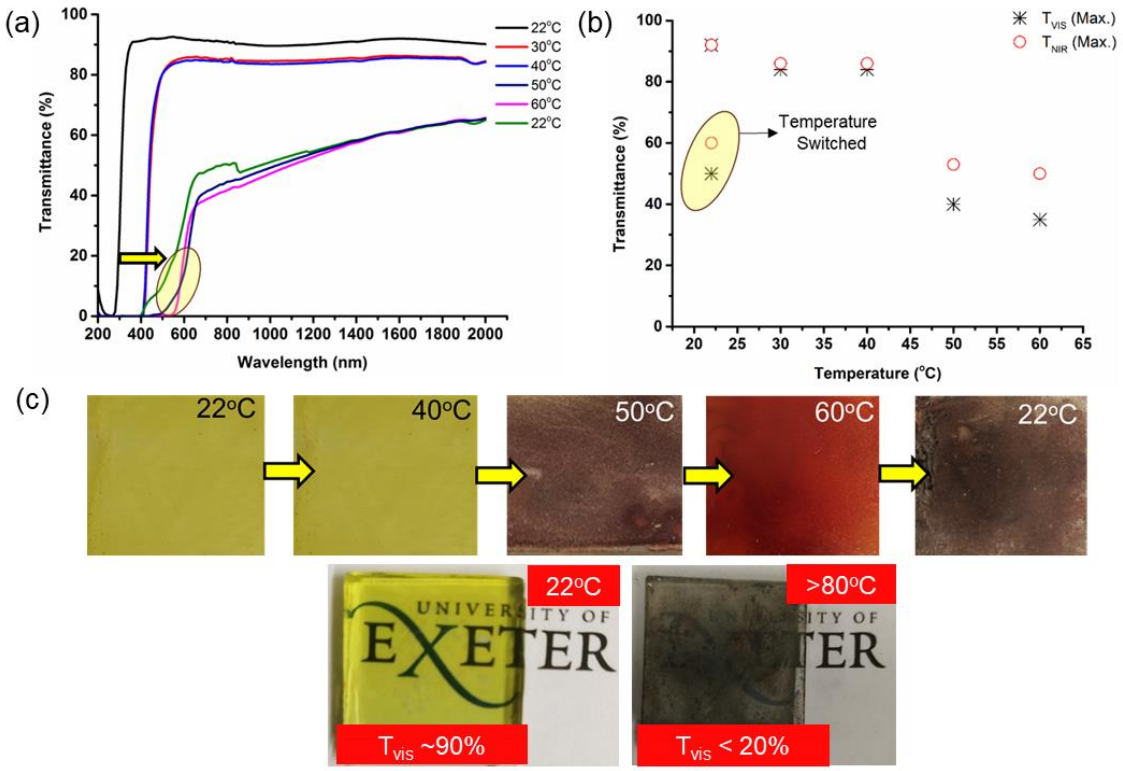

Figure 3. (a) Transmittance spectra of $MAPbIBr_2$ perovskite coating at their various thermal treatment, (b) a plot of maximum transparency observed for visible and near infrared at multiple temperatures of the $MAPbIBr_2$ perovskite coating, and (c) photograph of a gradual switching thermochromic $MAPbIBr_2$ perovskite coating.

4.2. Semi-switchable Thermochromic Property Investigation of the Perovskite Film. The coating colour was initially yellow (22^{o}C), followed by dark brown (40^{o}C) and finally attained in maroon colour (60^{o}C) during the thermal treatment. Interestingly, a similar colour is not achieved during the temperature switching from a high temperature to a modest temperature and lost transparency. The digital photographs of perovskite coatings further corroborated with **Figure 4a**. The hysteresis loop in the heating/cooling cycles of the perovskite coating was further examined. Perceiving the hysteresis loop is required to explain the perovskite material's transition process. The transition hysteresis of a TC material is always considered to have a detrimental effect on performance. Because the hysteresis loop exists, the absolute T_t will deviate from the average temperature. The transmittance and hysteresis loops of perovskite coatings (at 550 nm wavelength) have been collected under variable temperatures at intervals of 2°C and are shown in **Figure 4a**. This phenomenon can be attributed to the energy barrier being different between the heating and cooling processes (reversible dehydration and hydration process). Transmittance at the wavelength of 550 nm was selected to monitor the TC effect since the most significant difference in perovskite transmittance is observed at 550 nm. Simultaneously, 550 nm also corresponds to the peak in CIE photopic luminous human eye efficiency.[5] In this case, we observed that the transmission is not fully switchable and consisting of a broader loop. A slight average temperature difference is desirable. Simulation studies suggest that reducing the hysteresis loop's width can improve the energy savings to some degree.[5, 29] However, this result gives a preliminary indication of the switchable TC transmission property. After switching the temperature, we observed the maximum transparency value of ~35% at 35^{o}C, and of course, it is not entirely switchable. Further, the transparency declines as the temperature switched to 22^{o}C (expected to be increased), probably due to perovskite degradation resulting in a sharp bathochromic shift. **Figure 4b** reveals the visible

luminous transmittance (T_{vis}) and solar modulation ability (T_{sol}) of the perovskite thermochromic coating. A sinusoidal trend of both properties is observed. The T_{sol} varies across the temperature and has the highest value, 75%, at 45°C.

After this temperature, T_{vis} and T_{sol} both drops, which make it suitable for hot condition. At high external ambient temperature, this material absorbs solar radiation and become warm and change the transmission. Changing colour will reject the incoming solar radiation, which could increase the building interior's discomfort level. Lowest T_{vis} and Tsol were ~15% and 25%, respectively, at 55°C. Interestingly, the T_{sol} and T_{vis} values and their changing trend are similar up to 45°C. However, there is a drastic difference between these two values at the higher temperature. However, it was prominent that T_{sol} was always higher than T_{vis}. Loss of transmission could be due to material degradation or strong absorption of the incident light.

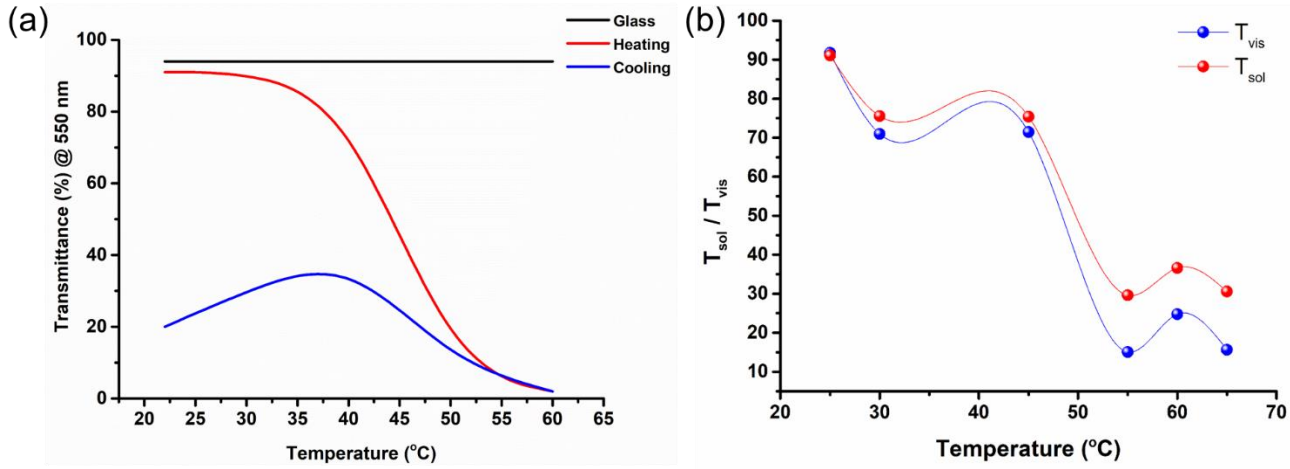

Figure 4. (a) The temperature-dependent thermochromic hysteresis loop (measured at 550 nm) of the $MAPbIBr_2$ perovskite window upon heating and cooling processes, and (b) plot of visible luminous transmittance (T_{vis}) and solar modulation ability (T_{sol}) against temperature for the thermochromic $MAPbIBr_2$ perovskite coating.

4.3. X-ray Diffraction Analysis of the Thermochromic Perovskite Film. Further, to understand the perovskite materials phase purity and stability, the thin film XRD analysis was performed, as shown in **Figure 5**. The intense predominant peaks of the $MAPbIBr_2$ perovskite coating observed at 23.44°, 24.53°, 28.33°, 31.86°, 40.43° and 43.09° correspond to the reflections of the (002), (112), (211), (202), (004), (312), (224) and (314) crystal planes of the tetragonal perovskite structure, respectively.[30] At room temperature, $MAPbI_3$ has a tetragonal phase, whereas $MAPbBr_3$ has a cubic phase. Consequently, $MAPb(I_{1-x}Brx)_3$ is known to undergo a phase transition from the tetragonal phase to the cubic phase for bromine doping > 20%.[31] A part of $MAPbIBr_2$ will be corroded by moisture, high temperature, and the degradation process's final products contain PbI_2 and $PbBr_2$. It is noted that no additional peaks related to PbI_2 were observed up to 40^{o}C. Once the temperature started to escalate and then switch from high to low temperature, there is a distinct (202) plane reflection, signifying the appearance of PbI_2, and similarly, many other small intensity PbI_2 peaks at higher theta positions. An interesting facet of this study is that the perovskite coating is almost phase pure and relatively stable with the same intensity up to 40^{o}C. As the temperature is extended, a part of the perovskite material started degraded to PbI_2 ($PbBr_2$). Also, the PbI_2 peak intensifies once it reaches 22^{o}C after the temperature switching. However, PbI_2 phase enhancement occurs (even at a lower temperature), probably due to the prolonged moisture interaction.[32] Thus, both temperature and moisture play a crucial role in such perovskite crystal stability. We find insignificant change was observed once the temperature was raised to 80 ^{o}C or lowered to 10^{o}C unless PbI_2 and $PbBr_2$ peak intensity enhancement **(Figure S1)**. The appearance of the PbI_2 phase facilitates increased exfoliation through the layer of the perovskite coating. The formation of this PbI_2 severely damages the performances of devices at very high and low-temperature regions.

Therefore, significant optical and structural characteristic changes were observed at a temperature between 10-60^{o}C for the $MAPbI_{3-x}Br_x$.

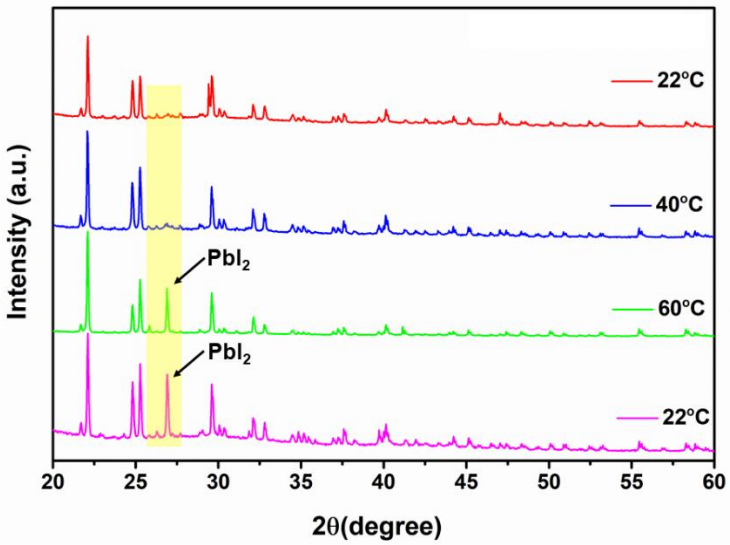

Figure 5. X-ray diffraction pattern of $MAPbIBr_2$ perovskite thin-film at different temperatures.

4.4. Scanning Electron Microscopic and Corresponding Elemental Analysis of the Thermochromic Perovskite Film. A part of the tetragonal $MAPbI_{3-x}Br_x$ will be corroded by moisture, high temperature, and the degradation process's final products contain PbI_2 and I_2. It is noted that no additional peaks related to PbI_2 were observed up to 40^{o}C. **Figure 6** represents the SEM microstructural images of the homogeneous perovskite coating for different temperatures. The SEM microstructural images of perovskite material exhibited densely packed elongated nanorods with a length of 1-3 µm and an average width of 10 ± 2 nm. SEM microstructural images of thermally treated $MAPbIBr_2$ perovskite film and their corresponding elemental mapping at 22^{o}C **(Figure 6a)**, 40^{o}C **(Figure 6b)**, 50^{o}C **(Figure 6c)**, and 60^{o}C **(Figure 6d)**, respectively are investigated. It appeared like these nanorods were laterally self-assembled to form a bundle-like pattern. In each bundle, similar types of nanorods are loosely held together. Besides the variation

of energy band structure, the morphologies of films may also affect the optical properties. For example, the increase in porosity resulted in a decrease in absorption coefficient; inhomogeneity is unlikely to affect the absorption edges significantly.

Interestingly, the nanorods' morphology and orientation remained intact for various thermal treatments and distributed homogeneously throughout the coating. Even after switching temperature, the nanorods features continued. Therefore, it is indispensable to inspect the perovskite material's elemental distribution during thermal treatment. The extensive area mapping ensures a homogeneous distribution of C, N, Pb, Br, and I, as the sole element present in the MAPbIBr2 film. The elemental mapping further confirms the homogeneous distribution of MAPbI3-xBrx throughout the film surface.

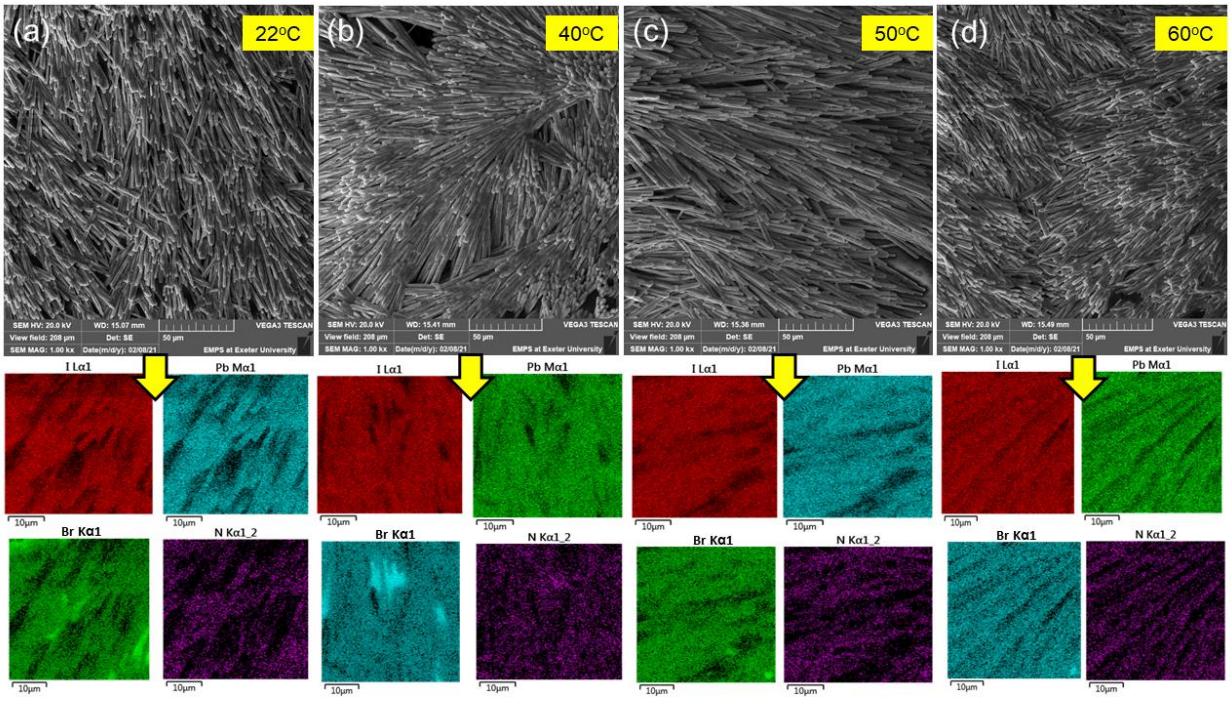

Figure 6. SEM microstructural images of thermally treated $MAPbIBr_2$ perovskite and their corresponding elemental mapping at (a) 22°C, (b) 40°C, (c) 50°C, and (d) 60°C, respectively.

4.5. Stability Performance of the Thermochromic Perovskite Film. The heating and cooling processes' kinetics are reported in **Figure 7a** for two various heat sources. Applying 1 SUN, the perovskite coating's chromic variation and heating-cooling cycle is shorter (42 min.) than the hotplate. It leads to a broad heating-cooling cycle, consuming 65 min to complete one cycle, keeping similar chromaticity of the perovskite coating. During cooling from 60 °C to room temperature, the chemical reactions step back, and the color of the mixture changes from marron to dark brown, and finally yellow. This result further interprets that the chromatic characteristics are independent of the heat source. In contrast, chromatic kinetics is dependent on the origin of heating/cooling. However, this process also does not restore the initial transparency and chromaticity, and therefore, is unable to offer complete switching or reversible chromaticity. Besides, as it has been observed from **Figure 2a**, there was a considerable bathochromic shift followed by a lower transmittance observed of the perovskite TC coating at the higher temperature; **Figure 7b** further reveals the absorbance values of the perovskite coating. It is considering the cold state (22-40^{o}C), the absorbance values relatively low and steady increment compared to their corresponding hot state (> 40^{o}C), where a substantial enhancement of absorption was observed, resulting in the maximum value of 0.83 at 60^{o}C, as measured up to 60 cycles. It is anticipated that the absorbance enhancement occurred due to the perovskite degradation, resulting in a degraded compound PbI_2, as shown in **Figure 5**.

On the other hand, the perovskite coating's stability at a particular temperature was also examined, as shown in **Figure 7c**. The maximum transmittance data has been recorded across the chromatic temperatures. Up to 60 cycles, the perovskite coating offers relatively steady transmission at their concerning temperature. After switching to 22^{o}C, the transmittance value (48%) is not dynamic, as observed up to 60 cycles. This result signifies that the perovskite coating exhibits static

transparency at a particular temperature and can be valuable several times. It is anticipated that the TC behaviour of perovskite crystals is dependent on their lattice structure deformation instead of changing of crystal structure induced by moisture and temperature.[33] Also, after switching the temperature from 60^{o}C to 22^{o}C, the resultant transparency signifies the perovskite cannot retain its as-prepared structure and therefore loses transparency. The incident light passes through at low temperature while strongly scatter the incident light at higher temperatures due to the formation of PbI_2 scattering centres of the aggregated nanorods.

Lin et al. (2018) suggested a substantial structural change occur in the perovskite structure upon phase transitions, often between a room-temperature non-perovskite phase and a high-temperature perovskite phase.[34] The phase transfer process drives off moisture (or assisted by extra heating), inducing a phase transition, while moisture ingress results in a subsequent phase transition back to the transparent low-T phase, as shown in **Figure 7d**. Besides, the TC behaviour of hydrated hybrid perovskite and attributed the thermochromism of perovskite to the reversible hydration/dehydration process encounters moisture. When these trapped holes are filled, entropy and lattice strain may cause the phase segregated material to relax back to the well-mixed alloy. Light-induced, reversible structural changes in $PbBr_2$ have been attributed to the self-trapping of such photogenerated holes.

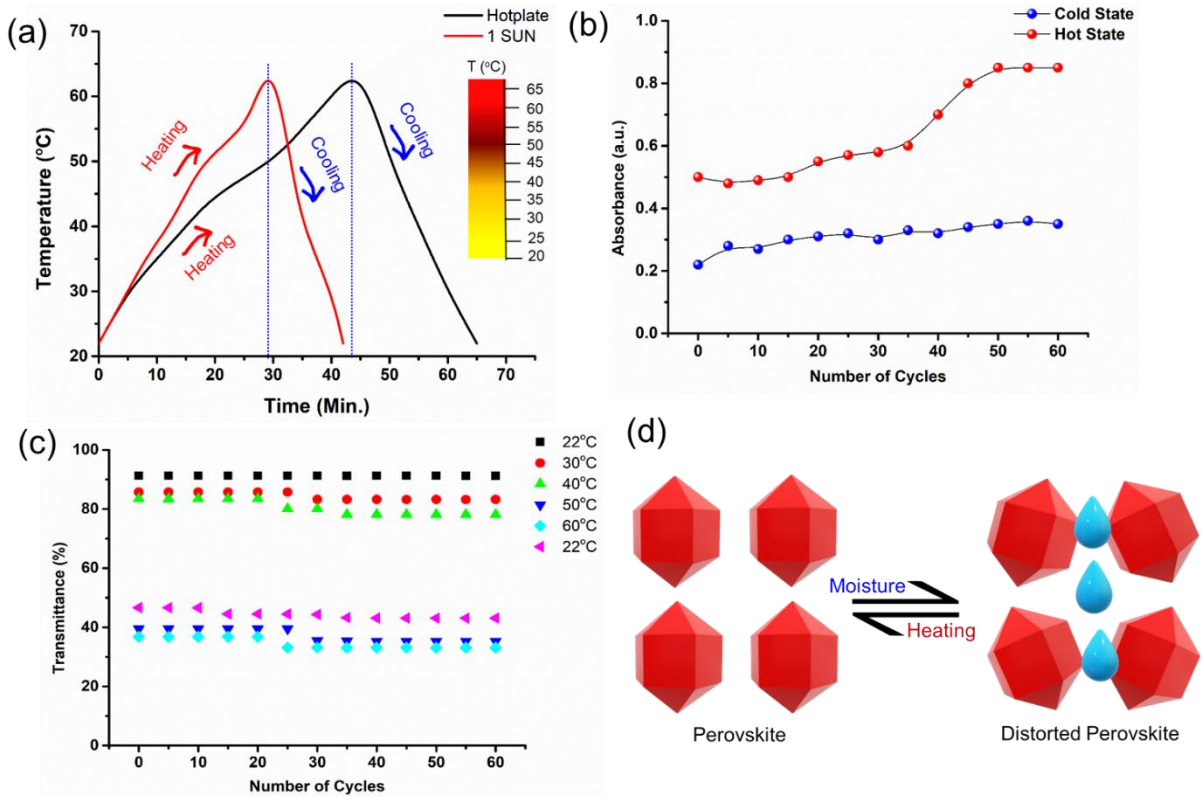

Figure 7. (a) The heating and cooling processes' kinetic plot are employing two various sources, (b) cycle testing plot in terms of their absorbance measurement, (c) cycle testing plot in a period of their transparency stability of the thermochromic $MAPbIBr_2$ perovskite coating for various temperatures, and (d) schematic presentation of reversible phase transition expelled by moisture and temperature.

4.6. Theoretical Investigation of the Thermochromic Perovskite Film. The calculated band structure of pure $MAPbI_3$ and its PDOS and optimized crystal structure is given in **Figure S2,** where the simulated bandgap (1.61 eV) has a good correlation with the observed one. Besides, this result is very consistent with the previously reported data of $MAPbI_3$, which validates and confirms our theoretical methodology.[35] As discussed in the experimental section, a range of Br as a doping agent has been applied to $MAPbI_3$, where $MAPbIBr_2$ exhibits attractive TC property; therefore, further, we are interested in analyzed theoretical modelling. The band structure of $MAPbIBr_2$, corresponding PDOS and crystal structures are depicted in **Figure 8a, Figure 8b,** and **Figure 8c,**

respectively**.** This result has also been compared with pure bulk $MAPbBr_3$, whose band structure, PDOS and crystal structure is given in **Figure S3**.

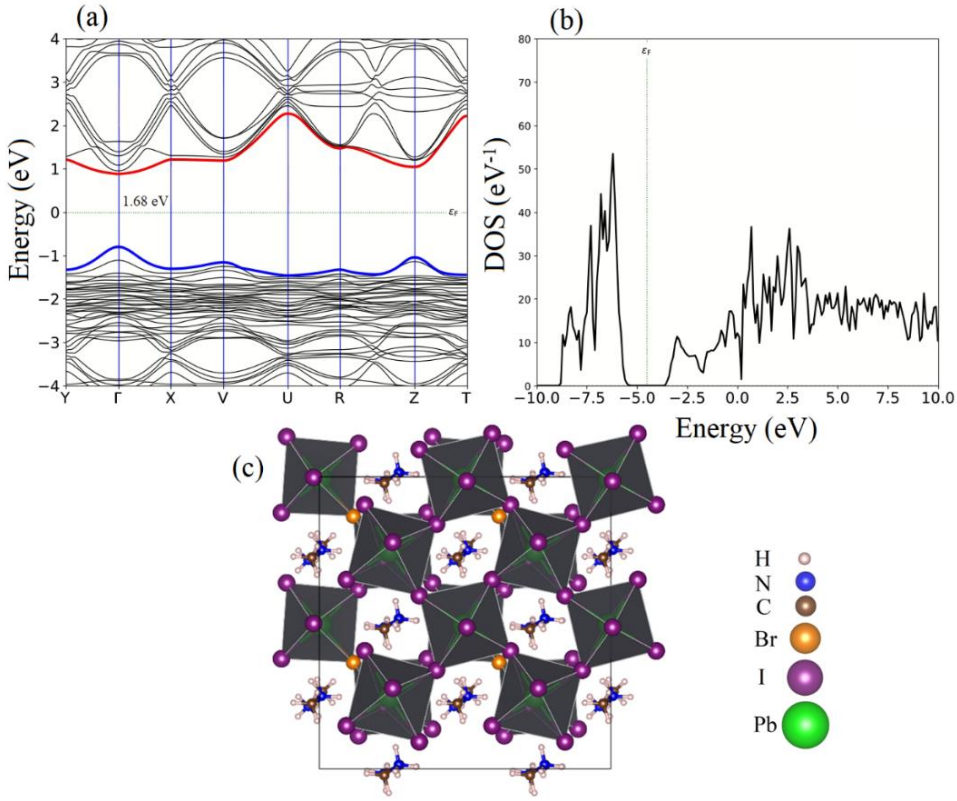

Figure 8. (a) Band structure, (b) PDOS and (c) crystal structure of bulk thermochromic $MAPbIBr_2$. The Fermi level of the band structure is fixed to zero.

Again, the simulated electronic properties of these two species are found to be coherent with the reported data.[34] In order to simplify our discussion, we focused on the $MAPbIBr_2$ and its water interacting system ($MAPbIBr_2$ (001) @ H_2O); hereafter will be denoted as $MAPbIBr_2@H_2O$. Upon interaction of water molecules with the surface of $MAPbIBr_2$, its crystal structure distorts. A comparative optimized relaxed geometry was investigated for $MAPbI_3$ **(Figure 9a)**, $MAPbIBr_2$ **(Figure 9b)**, (c) $MAPbBr_3$ **(Figure 9c)**, $MAPbI_3$ @ H_2O **(Figure 9d)**, $MAPbIBr_2$ @ H_2O **(Figure**

9e), and $MAPbBr_3$ @ H_2O **(Figure 9f)** for the (001) lattice plane. In addition, the bandgap of hydrated-$MAPbIBr_2$ reduces to 2.02 eV from 2.17 eV, as can be seen from **Figure S4**.

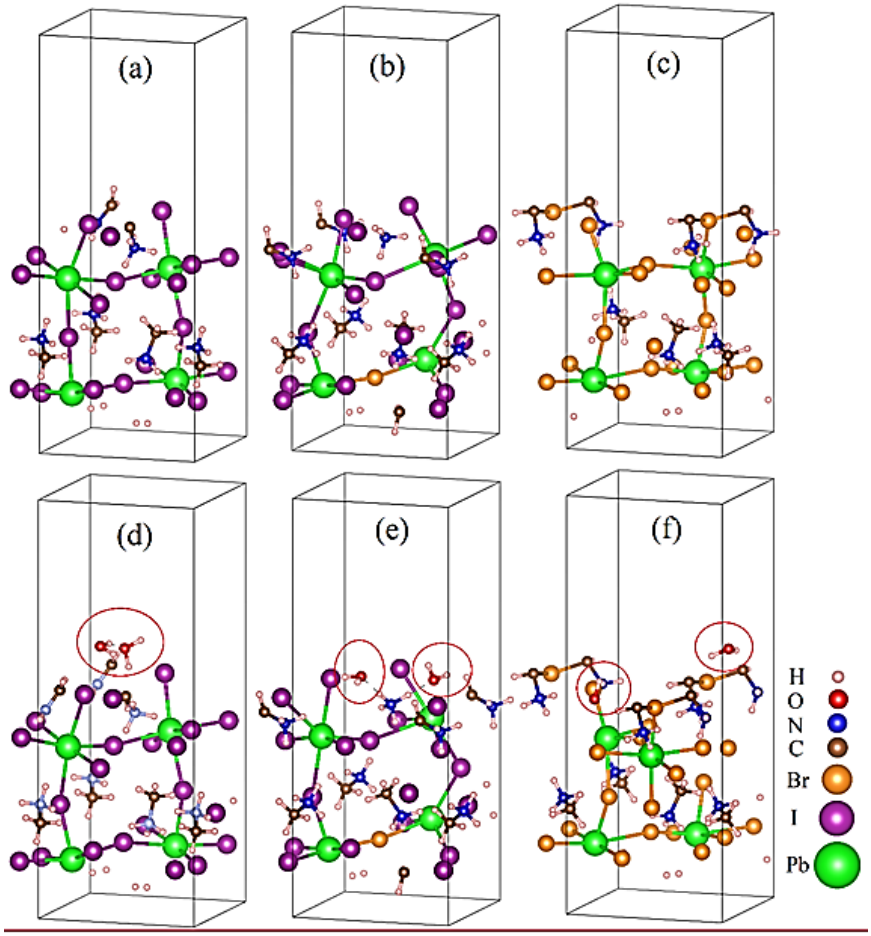

Figure 9. Optimized relaxed geometry of (a) $MAPbI_3$ (001), (b) $MAPbIBr_2$ (001), (c) $MAPbBr_3$ (001), (d) $MAPbI_3$ (001) @ H_2O, (e) $MAPbIBr_2$ (001) @ H_2O, and (f) $MAPbBr_3$ (001)@ H_2O, respectively.

This reduction in bandgap and crystal structure distortion depicts its increment in thermochromic nature compared to pristine one. Besides, this data strong corroborate our experimental ones. Furthermore, we also simulated and compared this moisture effect on $MAPbI_3$ and $MAPbBr_3$, as shown in **Figure 10** and **Table 1**. It can be analyzed from **Table 1** that $MAPbIBr_2$ has a strong

desire for water molecules in the form of -0.06 eV interaction energy compared to $MAPbI_3$ (0.50 eV) and $MAPbBr_3$ (0.33 eV). The distortion in the crystal structure of $MAPbIBr_2$ @ H_2O can also be seen from its electrostatic potential (ESP) map and 2D electron density difference maps, as shown in **Figure 10**. Comparative analysis of **Figure 10a** and **Figure 10b** led us to predict that water molecules have strong interaction with the surface of $MAPbIBr_2$. The moisture adsorbed on the perovskite surface may introduce vacancies into the crystal lattice and lowering the free-energy barrier to nucleation. The reason behind this strong interaction is the mutual sharing of electronic cloud density of water molecules with the surface of $MAPbIBr_2$. **Figure 10c** exhibits that upon the interaction of water molecules with $MAPbIBr_2$, its electron difference density map completely changed. Water molecules have disturbed the interface of $MAPbIBr_2$ (by exchange of electronic cloud density) and the whole bulk as well, where electron accumulation and donation occurred. So, this charge transfer (charge exchange) analysis further validates and confirms the superiority of $MAPbIBr_2$ @ H_2O over the non-hydrated species. In the presence of water, the perovskite may also get hydrated but can regain its original structure upon releasing the water molecules, which reveals their TC behaviour. From this study, it can be anticipated that moisture exposure effectively triggers the reversible hydration/dehydration process to the crystal structure of the hybrid perovskite at room temperature. This is further leading to a massive change in their bandgap, resulted in TC characteristics.

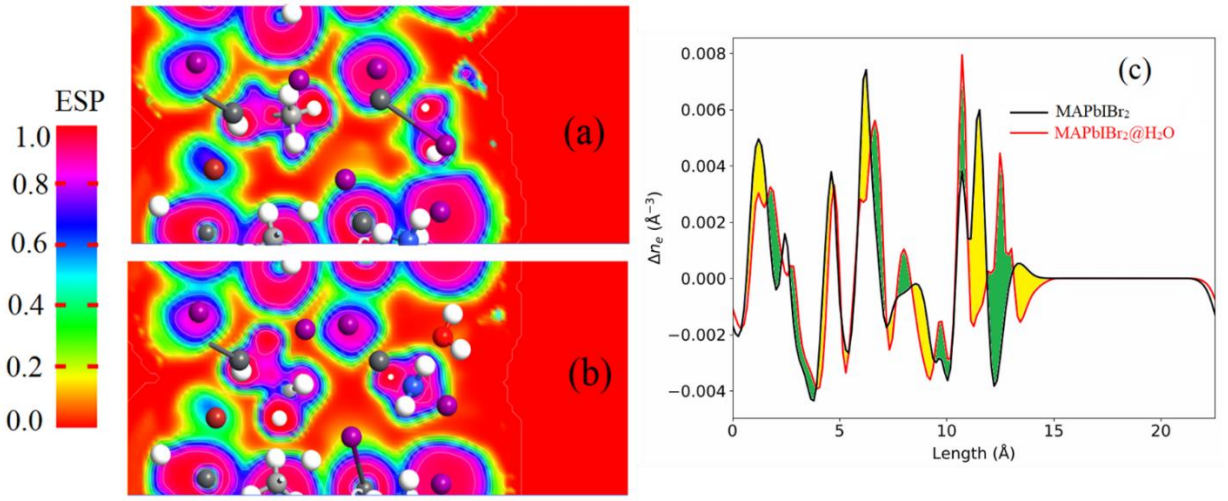

Figure 10. Electrostatic potential map (ESP) of (a) $MAPbIBr_2$ (001), (b), $MAPbIBr_2$ (001) @ H_2O, respectively, and (c) the electron density difference ($\Delta\rho$) in the Z-direction for $MAPbIBr_2$ (001) and its H_2O interacted system. The yellow and green shaded areas show electron accumulation and donation of $MAPbIBr_2$, respectively.

Table 1. Work function, bandgap, and water adsorption energy over the surface of $MAPbI_3$, $MAPbIBr_2$, and$MAPbBr_3$

Species	**Work function**	**Bandgap**	**$IntE_{H2O}$**
$MAPbI_3$	3.75	1.61	-
$MAPbI_3@H_2O$	-	-	+0.50
$MAPbIBr_2$	4.51	1.68	-
$MAPbIBr_2@H_2O$	-	-	-0.06
$MAPbBr_3$	4.25	2.41	-
$MAPbBr_3@H_2O$	-	-	+0.33

4.7. Thermal Comfort Analysis of the Thermochromic Perovskite Film. The perovskite coating's temperature measurements inside an insulated box have been measured using the thermocouples under 1SUN 1.5 AM. This experiment was carried out to perceive the perovskite coating's thermal comfort evolution for a window purpose. A schematic of the overall set-up for

the temperature measurements across the different parts of the prototype chamber is illustrated in **Figure 11a**. The perovskite coating's temperature profile has been further shown in **Figure 11b**. The TC perovskite coating effect was significantly enhanced when the glass surface temperature increased to 80^{o}C. Reflective glazing is more efficient during cooling seasons than absorptive (tinted) glazing as a part of the absorbed heat is later transferred to the building through convection. This indicates that the absorbed light facilitates a light-driven TC at a lower temperature, and as a result, the indoor temperature remains low.

In contrast, the inside temperature, considered a building inside temperature, is relatively low. Besides, after passing the perovskite chromatic T_t, the inside temperature started decreasing, resulting in an opaque state; even during the cooling process, the indoor temperature remains almost similar as recorded up to 200 min. The maximum temperature difference has been recorded at 50^{o}C when the outside temperature reaches 80^{o}C. The TC perovskite coating diminishes the ΔT to be minimized and retain this for a long time, as observed up to 200 min. A higher surface temperature difference indicates improved thermal insulation. This observation shows quite the impressive performance of TC perovskite coating as a glazing material to diminish the indoor temperature.

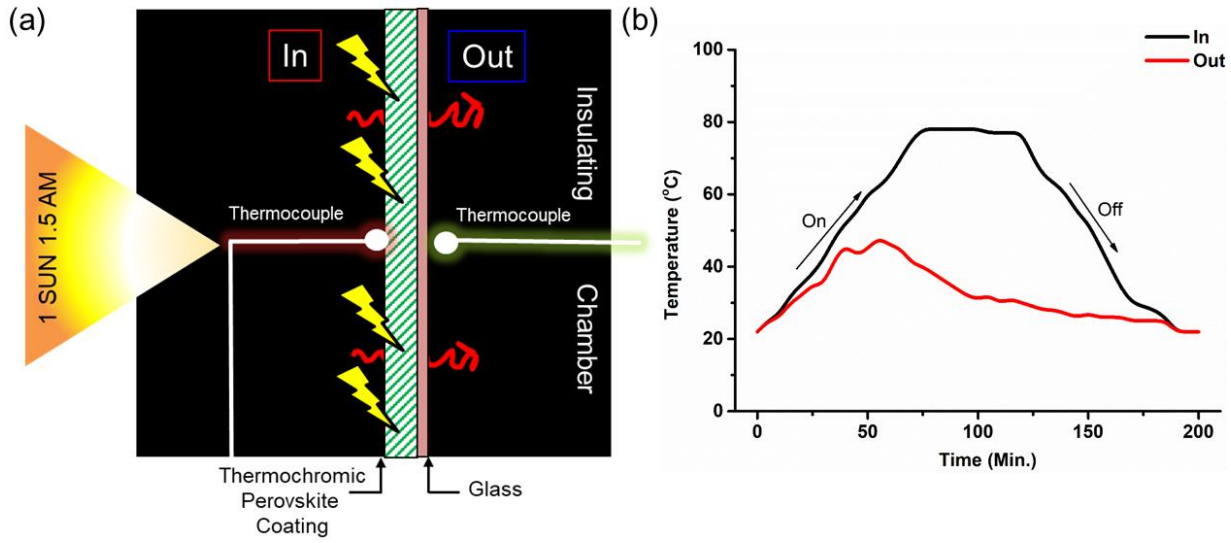

Figure 11. (a) Schematic diagram of the thermochromic $MAPbIBr_2$ perovskite coating-based prototype-glazing chamber under 1 SUN 1.5 AM condition, and (b) temperature profile plot of the thermochromic perovskite coating for simulator on and off situation. The simulator was turned off when the surface temperature becomes saturated.

We find the experimental factors associated with the results mentioned above are synthesis, nanorod formation, thermochromatic, phase stability, and thermal performance. The "hot-injection" method approach provides a large-scale synthesis of perovskite nanorods.[36] The SEM results show homogeneous growth and distribution of the perovskite nanorods with anisotropic growth. Moreover, due to their superior one-dimensional structure and reduced grain boundaries, nanorods are expected to favour a direct light-transmitting pathway. This is one of the effective methods to increase quantum efficiency by accumulating maximum light through the scattering and anti-reflection effect of the nanorods.[37] It can impressively reflect the passing light to the perovskite light absorber for round-trip absorption in turn, which is evidenced by higher transmittance values in the NIR region. Well-matched morphology with similar size and shape makes it possible to effectively propagate the heat in the films without additional energy loss

Besides, at a hot state, the perovskite coating allows more extended absorption of visible light due to a sort of degradation.

Perhaps, the extensive cycling test and semi-switchable properties of the perovskite coating promise futuristic employment in glazing. However, the perovskite coatings' stability is questionable and does not fit the cooler climates. Therefore, the chromaticity cycle is unable to evidence a complete switchable property. Besides, TC windows' energy simulation also highlights that this type of glazing is more efficient in warmer temperatures.

Nevertheless, due to their poor stability, high toxicity, and related environmental impact of lead (Pb) leakage, progress towards commercialization of the perovskite PV technology has been retarded. Pb is carcinogenic and has no safe threshold limit of exposure. Pb in the perovskite material can cause severe toxicological implications on the environment, dramatically impacting human health.[38, 39] Even modifying the structure and further protection (encapsulation) of the perovskite absorber layer cannot prohibit the risk of Pb leakage into the environment. In this stage, searching for better non-toxic alternative candidates is highly demanding. In this stage, searching for better non-toxic alternative candidates is highly challenging.

Interestingly, the flexible perovskite crystal structure admits a staggering number of elements with a wide variety of configurations.[40-42] A few of them have already reached marketing readiness, and undoubtedly, others will follow shortly.[43] Undoubtedly, VO_2 becomes a superior TC material for the window. However, it is difficult to improve further and accelerate its performance incorporating various technologies, such as multi-layered structure, porous film, composite film, etc. Besides, hydrogel and ionogel candidates are introduced for energy-efficient smart windows, but they stipulate encapsulation and suffer long time stability. Perovskite TCs have positioned a

good foundation for this work. Instead, the toxic impact of Pb will be an excellent approach to develop Pb-free TC perovskite windows that can be expected to influence energy use and efficiency significantly.[44-47] This study attempted to understand the TC behaviour and the initial impact of $MAPbI_{3-x}Br_x$ perovskite for window utilization. However, entire switching, high transparency, and stability is still a significant concern that can be rectified in the futuristic study.

Besides, there are still a few key challenges to be overcome: (1) improvement of the switchable thermochromic property (as minimum heating-cooling hysteresis), (2) engineering of the perovskite composition and structural modification to lower the transition temperature as well as control of thermal transmittance, (3) stability and long-term use of the TC coating, and (4) perhaps replacement of Pb for deployment in certain markets. Computational and experimental material design challenges are required to be addressed shortly. The correct management of solar gains is essential, contributing to heat in the indoor spaces, thus inducing a cooling load in summer, especially in passive buildings. In this regard, thermochromic glazing assisted building significantly shows a promising contribution for passive building thermal management. We believe our study opens the avenue of TC perovskite glazing implementation in future research.

5. CONCLUSIONS

In conclusion, mixed halide hybrid perovskite nanorods, $CH_3NH_3PbIBr_2$, were synthesized using the hot-injection method. Bromine addition was varied to get the composition $CH_3NH_3PbI_{3-x}Br_x$ started x = 0 to 3 at an interval of 1. Interestingly, the perovskite $CH_3NH_3PbIBr_2$ composition exhibits semi-switchable gradual thermochromic characteristics for a temperature window of 22-60^oC among the other composition and further selected for the study. The perovskite coating proclaims a periodic thermochromic starting from yellow (22^oC), reddish-brown (40^oC) and finally

maroon (60^{o}C), consisting of comparability modest T_t (40^{o}C), and offering semi-switchable property. Besides, the perovskite TC coating's transparency level excels 90% to 20% across the temperature window 22-60^{o}C. The experimental results signified the good thermal comfort behavior of the proposed material. Besides, the density functional theory was studied for three different types of models, i.e., pure $MAPbI_3$, 2%-Br-doped $MAPbI_3$ ($MAPbIBr_2$), and $MAPbBr_3$. Through simulation, it has been found that the 2D slabs of $MAPbI_3$, $MAPbIBr_2$ and $MAPbBr_3$ along [001] direction is constructed to predict the effect of water/moisture. The result further signifies that the crystal structure of $MAPbIBr_2$ shows a significant change in their crystal structure followed by band alignment once it interacts with water. Upon the interaction of water molecules with $MAPbIBr_2$, its electron difference density map completely reversed and changed compared to $MAPbI_3$ and $MAPbBr_3$. This may be a strong reason for the origin of mixed halide perovskite TC behaviour. Both the experimental and theoretical findings allow us to lower the TC point towards room temperature, applying the hybrid perovskites in smart windows. We presume that a few more of these TC perovskites with desired optoelectronic properties will be realized experimentally within the next few years. Many of the perovskites have the advantages of a strong absorption coefficient, substantial optoelectronics property, tunable low bandgap, ease to synthesize. However, Pb inclusion and perovskite's thermal and aqueous stability are significant issues and require further investigation for its complete glazing utilization. A more realistic approach has to be further explored when these results will be compared with the theoretical results of space-heating performance when replacing traditional TC glazed windows with mixed halides TC perovskite windows.

ASSOCIATED CONTENT

Supporting Information

XRD pattern of $MAPbIBr_2$ film (treated at 80°C), Band structure, PDOS and crystal structure of bulk pure $MAPBI_3$, $MAPBBr_3$ and $MAPbIBr_2$ @ H_2O, respectively.

AUTHOR INFORMATION

Corresponding authors

Anurag Roy - Environment and Sustainability Institute, University of Exeter, Penryn Campus, Cornwall TR10 9FE, U.K. Email: A.Roy30@exeter.ac.uk; ar.chem30@gmail.com

ORCID : https://orcid.org/0000-0002-2097-9442

Tapas K. Mallick - Environment and Sustainability Institute, University of Exeter, Penryn Campus, Cornwall TR10 9FE, U.K. Email: t.k.mallick@exeter.ac.uk

ORCID: https://orcid.org/0000-0002-6456-9955

Authors

Habib Ullah - Environment and Sustainability Institute, University of Exeter, Penryn Campus, Cornwall TR10 9FE, U.K. Email: hu203@exeter.ac.uk

Aritra Ghosh - Environment and Sustainability Institute, University of Exeter, Penryn Campus, Cornwall TR10 9FE, U.K. Email: a.ghosh@exeter.ac.uk

Hasan Baig - Environment and Sustainability Institute, University of Exeter, Penryn Campus, Cornwall TR10 9FE, U.K. Email: h.baig@exeter.ac.uk

Senthilarasu Sundaram - Environment and Sustainability Institute, University of Exeter, Penryn Campus, Cornwall TR10 9FE, U.K. Email: s.sundaram@exeter.ac.uk

Asif Ali Tahir - Environment and Sustainability Institute, University of Exeter, Penryn Campus, Cornwall TR10 9FE, U.K. Email: a.tahir@exeter.ac.uk

Notes

The authors declare no conflict of interest.

ACKNOWLEDGEMENTS

To carry out this work, financial support was provided by Engineering and Physical Sciences Research Council (EPSRC), the U.K. under research grant no. EP/T025875/1. The project's funders were not directly involved in the writing of this article. The authors acknowledge the help rendered for the XRD and SEM characterization by Dr Hong Chang, Imaging Suite Manager, Harrison Building, University of Exeter, Streatham Campus, North Park Road, Exeter, EX4 4QF, U.K.

REFERENCES

(1)Mahapatra, A.; Prochowicz, D.; Tavakoli, M.M.; Trivedi, S.; Kumar, P.; Yadav, P. A Review of Aspects of Additive Engineering in Perovskite Solar Cells. *J. Mater. Chem. A* **2000**, *8*, 27-54.

(2)Bhandari, S.; Roy, A.; Ghosh, A.; Mallick, T.K.; Sundaram, S. Perceiving the Temperature Coefficients of Carbon-Based Perovskite Solar Cells. *Sustain. Energ. Fuels* **2020**, *4*, 6283-6298.

(3)Bastiani, M.D.; Saidaminov, M.I.; Dursun, I.; Sinatra, L.; Peng, W.; Buttner, U.; Mohammed, O.F.; Bakr, O.M. Thermochromic Perovskite Inks for Reversible Smart Window Applications. *Chem. Mater.* **2017**, *29*, 3367-3370.

(4)Zhou, Y.; Cai, Y.; Hu, X.; Long, Y. Temperature-Responsive Hydrogel with Ultra-Large Solar Modulation and High Luminous Transmission for "Smart Window" Applications. *J. Mater. Chem. A* **2014**, *2*, 13550-13555.

(5) Zhang, Y.; Tso, C.Y.; Iñigo, J.S.; Liu, S.; Miyazaki, H.; Chao, C. Y.H., Yu, K. M. Perovskite Thermochromic Smart Window: Advanced Optical Properties and Low Transition Temperature. *Appl. Energy* **2019**, *254*, 113690.

(6)Wheeler, L.M.; Moore, D.T.; Ihly, R.; Stanton, N.J.; Miller, E.M.; Tenent, R.C.; Blackburn, J.L.; Neale, N.R. Switchable Photovoltaic Windows Enabled by Reversible Photothermal Complex Dissociation from Methylammonium Lead Iodide. *Nat. Commun.* **2017**, *8*, 1722.

(7)Minch, R.; Moonoosawmy, K. R. ; Solterbeck, C-H. ; Es-Souni, M. The Influence of Processing Conditions on the Morphology and Thermochromic Properties of Vanadium Oxide Films. *Thin Solid Films* **2014**, *556*, 277-284.

(8) Hoke, E.T.; Slotcavage, D.J.; Dohner, E.R.; Bowring, A.R.; Karunadasa, H.I.; McGehee, M.D. Reversible Photo-Induced Trap Formation in Mixed Halide Hybrid Perovskites for Photovoltaics. *Chem. Sci.* **2015**, *6*, 613-617.

(9) Tombe S.; Adam, G.; Heilbrunner, H.; Apaydin, D.H.; Ulbricht, C.; Sariciftci, N.S.; Arendse, C.J.; Iwuoha, E.; Scharber, M.C. Optical and Electronic Properties of Mixed Halide (X = I, Cl, Br) Methylammonium Lead Perovskite Solar Cells. *J. Mater. Chem. C*, **2017**, *5*, 1714-1723.

(10) Hong, K.; Le, Q.V.; Kim, S.Y.; Jang, H.W. Low-dimensional Halide Perovskites: Review and Issues. *J. Mater. Chem. C* **2018**, *6*, 2189-2209.

(11) Liu, P.; He, X.; Ren, J.; Liao, Q.; Yao, J.; Fu, H. Organic-Inorganic Hybrid Perovskite Nanowire Laser Arrays. *ACS Nano* **2017**,*11*, 5766-5773.

(12) Sayfouri, M.M.; Binions, R. Sol-gel Approaches to Thermochromic Vanadium Dioxide Coating for Smart Glazing Application. *Sol. Energy Mater. Sol. Cells* **2017**, *159*, 52-65.

(13) Cui, Y.; Ke, Y.; Liu, C.; Chen, Z.; Wang, N.; Zhang, L.; Zhou, Y.;Wang, S.; Gao, Y.; Long, Y. Thermochromic VO_2 for Energy-Efficient Smart Windows. *Joule* **2018**, *2(9)*, 1707-1746.

(14) Fleer, N. A.; Pelcher, K. E.; Nieto, K.; Braham, E.J.; Zou, J.; Horrocks, G.A. Naoi, Y.; Depner, S.W.; Schultz, B.J.; Amano, J.; Sellers, D.G.; Banerjee, S. Elucidating the Crystallite Size Dependence of the Thermochromic Properties of Nanocomposite VO_2 Thin Films. *ACS Omega* **2018**, *3(10)*, 14280-14293.

(15) Sayfouri, M.M.; Binions, R. Sol-gel Approaches to Thermochromic Vanadium Dioxide Coating for Smart Glazing Application. *Solar Energy Mater. Solar Cells* **2017**, *159*, 52-65.

(16) Liang, X.; Chen, M.; Wang, Q.; Guo, S., Zhang, L.; Yang, H. Active and Passive Modulation of Solar Light Transmittance in a Hybrid Thermochromic Soft-Matter System for Energy-Saving Smart Window Applications. *J. Mater. Chem. C* **2018**,*6*, 7054-7062.

(17) Zhou, Y.; Dong, X.; Mi, Y.; Fan, F.; Xu, Q.; Zhao, H.; Wang, S.; Long, Y. Hydrogel Smart Windows. *J. Mater. Chem. A* **2020**, *8*, 10007-10025.

(18) Cheng, Y.; Zhang, X.; Fang, C.; Chen, J.; Wang, Z. Discoloration Mechanism, Structures and Recent Applications of Thermochromic Materials via Different Methods: A Review. *J. Mater. Sci. Technol.* **2018**, *34*, 2225-2234.

(19) Sadhukhan, P.; Kundu, S.; Roy, A.; Ray, A.; Maji, P.; Dutta, H.; Pradhan, S.K.; Das, S. Solvent-Free Solid-State Synthesis of High Yield Mixed Halide Perovskites for Easily Tunable Composition and Band Gap. *Cryst. Growth Des.* **2018**, *18*, 3428-3432.

(20) Jang, D. M.; Park, K.; Kim, D. H.; Park, J.; Shojaei, F.; Kang, H. S.; Ahn, J. P.; Lee, J. W.; Song, J. K. Reversible Halide Exchange Reaction of Organometal Trihalide Perovskite Colloidal Nanocrystals for Full-Range Band Gap Tuning. *Nano Lett.* **2015**, *15 (8)*, 5191-5199.

(21) Shamsi, J.; Urban, A.S.; Imran, M.; Trizio, L.D.; Manna, L. Metal Halide Perovskite Nanocrystals: Synthesis, Post-Synthesis Modifications, and Their Optical Properties. *Chem. Rev.* **2019**, *19 (5)*, 3296-3348.

(22) Huang, H.; Polavarapu, L.; Sichert, J.A.; Susha, A.S.; Urban, A.S.; Rogach, A.L. Colloidal Lead Halide Perovskite Nanocrystals: Synthesis, Optical Properties and Applications. *NPG Asia Mater* **2016**, *8*, e328.

(23) Ghosh, A.; Norton, B. Advances in Switchable and Highly Insulating Autonomous (Self-Powered) Glazing Systems for Adaptive Low Energy Buildings. *Renew. Energy.* **2018**, *126*, 1003-1031.

(24) Ghosh, A.; Sundaram, S.; Mallick, T.K. Investigation of Thermal and Electrical Performances of a Combined Semi- Transparent PV-Vacuum Glazing. *Appl. Energy.* **2018**, *228*, 1591-1600.

(25) Hemaida, A.; Ghosh, A.; Sundaram, S.; Mallick, T.K. Evaluation of Thermal Performance for a Smart Switchable Adaptive Polymer Dispersed Liquid Crystal (PDLC) Glazing. *Sol. Energy* **2020**, *95*, 185-193.

(26) Roy, A.; Ghosh, A.; Benson, D.; Mallick, T.K.; Sundaram, S. Emplacement of Screen-Printed Graphene Oxide Coating for Building Thermal Comfort Discernment. *Sci. Rep.* **2020**, *10*, 15578.

(27) QuantumATK version Q-2019.12 *www.quantumatk.com*

(28) Enkovaara, J. e.; Rostgaard, C.; Mortensen, J. J.; Chen, J.; Dułak, M.; Ferrighi, L.; Gavnholt, J.; Glinsvad, C.; Haikola, V.; Hansen, H. Electronic Structure Calculations with GPAW: A Real-

Space Implementation of the Projector Augmented-Wave Method. *J. Phys: Condens. Matter.* **2010**, *22*, 253202.

(29) Yang, J.; Xu, Z.; Ye, H.; Xu, X.; Wu, X.; Wang, J. Performance Analyses of Building Energy on Phase Transition Processes of VO_2 Windows with an Improved Model. *Appl. Energy* **2015**, *159*, 502-508.

(30) Aharon, S.; Cohen, B.E.; Etgar, L; Hybrid Lead Halide Iodide and Lead Halide Bromide in Efficient Hole Conductor Free Perovskite Solar Cell. *J. Phys. Chem. C* **2014**, *118*, 17160-17165.

(31) Martynow, M.; Głowienka, D.; Galagan, Y.; Guthmuller, J. Effects of Bromine Doping on the Structural Properties and Band Gap of $CH_3NH_3Pb(I_{1-x}Br_x)_3$ Perovskite. *ACS Omega* **2020**, *5(41)*, 26946-26953.

(32) Gujar, T.P.; Unger, T.; Schönleber, A.; Fried, M.; Panzer, F.; Smaalen, S.; Köhler, A.; Thelakkat, M. The Role of PbI_2 in $CH_3NH_3PbI_3$ Perovskite Stability Solar Cell Parameters and Device Degradation. *Phys. Chem. Chem. Phys.* **2018**, *20*, 605-614.

(33) Ning, W.; Zhao, X.-G.; Klarbring, J.; Bai, S.; Ji, F.; Wang, F.; Simak, S.I.; Tao, Y.; Ren, X.-M.; Zhang, L.; Huang, W.; Abrikosov, I.A.; Gao, F. Thermochromic Lead-Free Halide Double Perovskites. *Adv. Functional Mater.* **2019**, *29 (10)*, 1807375.

(34) Lin, J.; Lai, M.; Dou, L.; Kley, C.S.; Chen, H.; Peng, F.; Sun, J.; Lu, D.; Hawks, S.A.; Xie, C.; Cui, F.; Alivisatos, A.P.; Limmer, D.T.; Yang, P. Thermochromic Halide Perovskite Solar Cells. *Nature Mater.* **2018**, *17*, 261-267.

(35) Amat, A.; Mosconi, E.; Ronca, E.; Quarti, C.; Umari, P.; Nazeeruddin, M. K.; Gratzel, M.; De Angelis, F. Cation-induced Band-Gap Tuning in Organohalide Perovskites: Interplay of Spin-Orbit Coupling and Octahedra Tilting. *Nano letters* **2014**, *14*, 3608-3616.

(36) Xu, H.; Wang, J.; Xuan, T.; Lv, C.; Hou, J.; Zhang, L.; Dong, Y.; Shi, J. Convenient and Large-Scale Synthesis of High-Quality, All-Inorganic Lead Halide Perovskite Nanocrystals for White Light-Emitting Diodes. *Chem. Eng. J.* **2019**, *364*, 20-27.

(37) Zhang, J.; Yang, X.; Deng, H.; Qiao, K.; Farooq, U.; Ishaq, M.; Yi, F.; Liu, H.; Tang, J.; Song, H. Low-dimensional Halide Perovskites and Their Advanced Optoelectronic Applications. *Nano-Micro Lett.* **2017**, *9*, 36.

(38) Hailegnaw, B.; Kirmayer, S.; Edri, E.; Hodes, G.; Cahen, D. Rain on Methylammonium Lead Iodide Based Perovskites: Possible Environmental Effects of Perovskite Solar Cells. *J. Phys. Chem. Lett.* **2015**, *6*, 1543-1547.

(39) Li, J.; Cao, H.L.; Jiao, W.B.; Wang, Q.; Wei, M.; Cantone, I.; Lü, J.; Abate, A. Biological Impact of Lead from Halide Perovskites Reveals the Risk of Introducing a Safe Threshold. *Nat. Commun.* **2020**, *11*, 310.

(40) Jena, A.K.; Kulkarni, A.; Miyasaka, T. Halide Perovskite Photovoltaics: Background, Status, and Future Prospects. *Chem. Rev.* **2019**, *119*, 3036-3103.

(41) Li, J.; Duang, J.; Yang, X.; Duan, Y.; Yang, P.; Tang, Q. Review on Recent Progress of Lead-Free Halide Perovskites in Optoelectronic Applications. *Nano Energy* **2021**, *80*, 105526.

(42) Li, J.; Liu, X.; Cui, P.; Li, J.; Ye, T.; Wang, X.; Zhang, C.; Zhao, Y.S. Lead-free Thermochromic Perovskites with Tunable Transition Temperatures for Smart Window Applications. *Sci. China Chem.* **2019**, *62*, 1257-1262.

(43) Chang, T.C.; Cao, X.; Bao, S.-H.; Ji, S.-D.; Luo, H.-J.; Jin, P. Review on Thermochromic Vanadium Dioxide based Smart Coatings: From Lab to Commercial Application. *Adv. Manuf.* **2018**, *6*, 1-19.

(44) Zhang, W.; Sun, Z.; Zhang, J.; Han, S.; Ji, C.; Li, L.; Hong, M.; Luo, J. Thermochromism to Tune the Optical Bandgap of a Lead-Free Perovskite-type Hybrid Semiconductor for Efficiently Enhancing Photocurrent Generation. *J. Mater. Chem. C* **2017**, *5*, 9967-9971.

(45) Batmunkh, M.; Zhong, Y.L.; Zhao, H. Recent Advances in Perovskite-based Building-Integrated Photovoltaics. *Adv. Mater.* **2020**, *6*, 2000631.

(46) Roy, A.; Ghosh, A.; Bhandari. S.; Sundaram, S.; Mallick, T.K. Perovskite Solar Cells for BIPV Application: A Review. *Buildings* **2020**, *10(7)*, 129.

(47) Long, L.; Ye, H. How to be Smart and Energy Efficient: A General Discussion on Thermochromic Windows. *Sci. Rep.* **2014**, *4*, 6427.

Table of Content

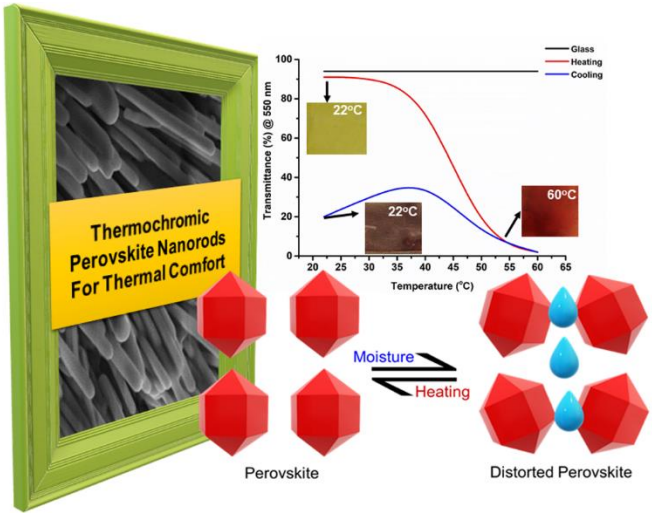

A hybrid mixed halide perovskite, $CH_3NH_3PbIBr_2$, has been employed as a thermochromic coating for window purposes. They employ TC perovskites in energy-efficient smart windows and other building technologies due to their significant absorption coefficient and color tunability.